

# NEBULIZERS: AERODYNAMIC DROPLET DIAMETER CHARACTERIZATION AND PHYSICOCHEMICAL PROPERTIES OF DRUGS TO TREAT SEVERE ACUTE RESPIRATORY SYNDROME CORONA VIRUS 2 (SARS-COV-2)



Walter Duarte de Araújo Filho <sup>\*1✉</sup>, Luciana Martins Pereira de Araújo <sup>2</sup>, Anderson Silva de Oliveira <sup>1,3</sup>, Vagner Cardoso da Silva <sup>4</sup>, Aníbal de Freitas Santos Júnior <sup>4</sup>



<sup>\*1</sup>Department of Exact and Earth Sciences, State University of Bahia, Salvador, Bahia, Brazil

<sup>2</sup>Jorge Amado University Center (UNIJORGE), Salvador, Bahia, Brazil

<sup>3</sup>Coordination of Surveillance, Investigation and Monitoring, Directorate of Sanitary and Environmental Surveillance of the State of Bahia, Salvador, Bahia, Brazil

<sup>4</sup>Department of Life Sciences, State University of Bahia, Salvador, Bahia, Brazil

DOI: <https://doi.org/10.29121/granthaalayah.v8.i7.2020.420>

**Article Type:** Research Article

**Article Citation:** Walter Duarte de Araújo Filho, Luciana Martins Pereira de Araújo, Anderson Silva de Oliveira, Vagner Cardoso da Silva, and Aníbal de Freitas Santos Júnior. (2020). NEBULIZERS: AERODYNAMIC DROPLET DIAMETER CHARACTERIZATION AND PHYSICOCHEMICAL PROPERTIES OF DRUGS TO TREAT SEVERE ACUTE RESPIRATORY SYNDROME CORONA VIRUS 2 (SARS-COV-2). International Journal of Research -GRANTHAALAYAH, 8(7), 80-97. <https://doi.org/10.29121/granthaalayah.v8.i7.2020.420>

**Received Date:** 02 June 2020

**Accepted Date:** 26 July 2020

**Keywords:**

Drugs  
SARS-Cov-2  
Nebulizers  
Direct Laminar Incidence  
Physicochemical Properties

**ABSTRACT**

Currently, several drugs are being used systemically to treat Severe Acute Respiratory Syndrome Coronavirus 2 (SARS-CoV-2). However, few studies discuss the possibility of using the inhalation route for this treatment. Pneumatic and ultrasonic nebulizers are increasingly used due to the ease with which these media deliver drugs through an aerosol suspension to deliver drugs in a localized manner in the respiratory tract, providing greater efficiency of absorption. This study aims to characterize the droplet diameters by bands of "breathable particles" generated by nebulizers commercialized in Brazil (2 pneumatic and 1 ultrasonic), using the direct laminar incidence (DLI) technique. In addition, to discuss the use of drugs by inhalation based on the physicochemical and pharmacology properties. In the nebulization procedure, the images of the dispersed aero droplets were captured using the DLI technique. Droplet diameter distribution histograms were elaborated, emphasizing the range of droplets with diameters between 1.0 to 5.0  $\mu\text{m}$ . The results attested that each nebulizer has its own characteristic of delivering the aerodynamic suspension in the nebulization process. In this study, DLI represents a viable alternative for characterization of the aero dispersed droplets, of drugs used worldwide to treat SARS-CoV-2 signs and symptoms.

## 1. INTRODUCTION

The interaction with the environment exposes human beings to several microorganisms, among which stand out viruses. There are more than 300,000 viruses hosted in mammals and about 200 of them are known to infecting humans [1], [2]. With the expansion of this contact, the increase in the frequency of emerging viral infections is notorious, such as Ebola [3], Zika [4], Severe Acute Respiratory Syndrome (SARS) [5] and, recently, in 2019, in China, the Coronavirus 2019-nCoV [6]. Thus, the search for new drugs and treatments is essential to avoid spread, especially in the Severe Acute Respiratory Syndrome Coronavirus 2 (SARS-CoV-2).

Currently, several drugs are being used systemically (oral or parenteral) to treat emerging viral infections, especially for SARS-CoV-2. However, there are no studies that directly discuss the possibility of using the inhalation route for this treatment. Physicochemical properties of drugs, such as water solubility, acid dissociation constant (pKa), oil/water partition coefficient, molecular mass, granulometry, surface contact area, among others, are essential for the development of pharmaceutical forms dispersible [7]. For inhalation application, the drugs must be efficient aerosolization and rapid dissolution of the drug crystals. [8].

In the last decades, aerosol therapy has achieved significant progress, which has determined that its use makes it a faster, more effective and safer modality for the treatment of various respiratory diseases [9], [10]. This form of administration allows the drug to arrive directly at the site of action, avoiding the need to use the digestive tract or parenteral route. The administration of drugs by inhalation offers the following advantages: possibility to use significantly less amount of drug; higher blood levels, with lesser side effects; and, faster action [11], [12].

In the respiratory tree, the greatest resistance occurs in the upper airways (lining of the mouth, tongue and oropharynx) due to the tendency of this region to retain large particles. This becomes an obstacle when it is desired that the particles carrying active drug penetrate the lower airways [13], [14]. The movement of particles is governed by two types of factors: the intrinsic of the aerosol and, those inherent to the patient.

One of the intrinsic factors of aerosol is the aerodynamic behaviour of particles in the respiratory system, governed mainly by size: The diameter of the particles is the most important factor in determining whether they can enter the lower airway and reach the site of action [15], [16]. Very small particles (less than 1.0  $\mu\text{m}$ ) have low drug transport capacity and a high probability of being exhaled into the environment without reaching the respiratory epithelium. Very large particles (> 5.0  $\mu\text{m}$ ) have a high tendency to agglomerate and quickly impact the upper airway; therefore, they are associated with the possibility of generating greater systemic effects. Particles of intermediate size, 1.0 to 5.0  $\mu\text{m}$ , are "ideal" because, through deposition, sedimentation and diffusion mechanisms, they can reach the walls of the lower airways [17]. Particles with this characteristic constitute the "breathable mass" of an aerosol. Therapeutic aerosols are "polydispersed", which means that the aerosol cloud is made up of particles of very different sizes [18], [19]. As the dispersion is asymmetric (non-Gaussian), an aerosol can be characterized in terms of a central measure of trend, the mass means aerodynamic diameter (MMAD) and a dispersion measure, the geometric standard deviation (GSD). For the administration of particles in the peripheral pathways, the system that provides an aerosol with the smallest MMAD and the narrowest GSD will be the most suitable.

In addition, other intrinsic aerosol factors are relevant, such as, input speed: the higher the speed, the greater the likelihood of deposition in the upper airways; electrostatic charge: the influences of attraction and repulsion by the electric charge can be between the particles, or between the particles and the airway walls; and, Hygrophilicity: It is the property of particles to increase in size when they are in an environment saturated with water, such as the airway. It can be seen that due to the size, some types of drugs are "inefficient", because a large part is wasted on the route not reaching the action site for the procedure to be effective [20]. It is noted that part of the dose inhaled by the patient is divided into droplets that can be larger or smaller than 5.0  $\mu\text{m}$ ; for those larger than 5.0  $\mu\text{m}$  that are deposited in the upper airways, there is digestive absorption that culminates in systemic effects and renal excretion.

For droplets smaller than 5.0  $\mu\text{m}$  there is a deposition in the lower airways leading to the expected therapeutic effect. The proportion of particle distribution in the respiratory system depends on the type of generation method and on the countless variables that participate in its performance characteristics [21]. Based on what was previously treated, the size of the droplets generated in the nebulization process has a crucial role in the effectiveness of the drug's action during treatment [22]. The design of each nebulizer has specific characteristics that make them behave differently in the nebulization process [23].

Reference techniques are used for characterizing droplet size, such as, Laser diffraction (LD), Cascade impactor and Phase doppler anemometry (PDA). In Laser Diffraction (LD) technique, the particles present in the aerodynamic

suspension absorb or disperse light incident according to its size, shape and refractive index. The scattered light is subsequently collimated by the lenses of a Fourier transformer, and focused on a detector on the center axis positioned at a distance from the lens equivalent to the focal length. The non-diffracted light is focused on the central detector. In this way, a diffraction pattern of all contributing particles is recorded as a function of the dispersion angle [24], [25].

The technique based on inertial behaviour, also known as Cascade Impactor (CI), also represents one of the ways to measure the diameter of the droplets in suspension aerodynamics. This method is based on particle inertia and is used to characterize aerosols through a device where the particles are separated by impact at various levels. The current of air that entrains the particles is accelerated through a nozzle against a flat plate. The gas current lines change abruptly, which does not happen with some particles, especially the larger ones, which, due to their high inertia, precipitate in the dish. The passage of the particles through successive stages causes their deposition in fractions with successively smaller diameters. In each floor mass fractions of particles are obtained with the same inertia, that is, the same aerodynamic diameter, which, after mathematical manipulation, generated the size distribution of the initial sample [26], [27].

PDA is one of the most accurate for the characterization of particle size in aerodynamic dispersion. In this technique, several detectors positioned at different scattering angles are used to sample slightly different spatial portions of the scattered light signal per particle. A system of two-phase shift detectors transmits information about the particle diameter, shrinkage index and geometric shape characteristics. PDA is capable of characterizing particles of wide dynamic size, from 0.3 to 8.0  $\mu\text{m}$ , with an accuracy of 5% [28].

Thus, there is a problem to be answered: How to quantify the efficiency of nebulizers in delivering dispersed aero droplets with diameters in the range between 1.0 and 5.0  $\mu\text{m}$  (breathable droplets)? In search of an answer to this question, DLI technique was used to characterize the population of droplets generated in the nebulization process, emphasizing the region between 1.0 and 5.0  $\mu\text{m}$ , which corresponds to the ideal range absorption of the drug in the lower respiratory tract, which allows a better response to therapeutic treatment.

In the current pandemic scenario of the SARS-CoV-2, this paper presents a method to measure the diameter of droplets generated by nebulizers in misting procedures by DLI technique. This paper also discusses the possibility of using drugs by nebulizers, based on the physicochemical properties of drugs already used in clinical practice.

## 2. MATERIALS AND METHODS

### 2.1. NEBULIZERS AND DROPLETS IN AERODYNAMIC SUSPENSION

In the development of the work, three household nebulizers were randomly chosen, commercialized in the Brazilian market, two pneumatic and one ultrasonic. They will be designated by the letters A, B and C. To quantify the droplet size, a Stage Micrometer (Edmund Optics. 30-101, USA) was used, attached to the eyepiece of the Axiovert A1 tri-eyed microscope (Carl Zeiss, Jena, Germany). The images were obtained using a high-speed digital camera (HiSpec 47; Fastec Imaging) with a resolution of 1696 x 1710 pixels, at an acquisition rate of 200 fps.

A 0.9% saline solution was used to constitute the aqueous vehicle of the nebulizers, with an estimated viscosity of 0.90 mPa. The images were obtained by directly focusing the aerosol generated on a glass slide coupled to the microscope at a fixed distance of 0.1, at a temperature of 22o C, atmospheric pressure of 102.1 kPa, and with relative humidity of the air around 68%.

The images of the droplets close to the slide were captured and stored in a memory unit. They were acquired at a rate of 200 (fps) with a total acquisition time of 2 s, totalling 400 images for each researched nebulizer by LDI technique. Figure 1 presents an image obtained from a population of droplets flush with the slide, excluding the droplets condemned on its surface. The image was acquired with a 200X increase, an acquisition rate of 200 fps, a temperature of 22o C, an atmospheric pressure of 102.1 kPa and a relative humidity of around 68%.

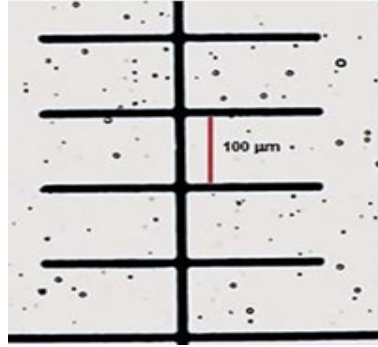


**Figure 1:** Image of droplets in aerodynamic suspension acquired by the experimental device. Source: Own authorship.

To quantify the size of the droplets, the images were processed using a protocol established in MATLAB® version 2015b.

## 2.2. IMAGE PROCESSING USED IN THE ACQUISITION OF EXPERIMENTAL DATA

The first step in processing was to segment the images. The objective was to try to differentiate all the regions that represent the droplets from the rest of the image. This segmentation is done by comparing the image to be processed with a reference image (image from the same region filmed during the experiment, but without the presence of droplets). An example of a real image (a) next to a reference image (b) can be seen in Figure 2.

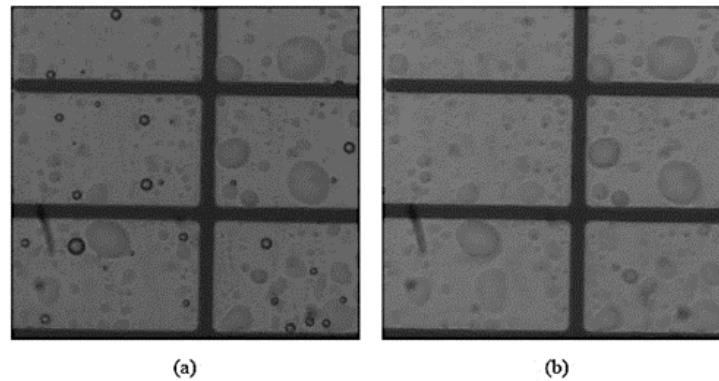


**Figure 2:** (a) Image to be processed (b) Reference image. Source: Own authorship.

All pixels of the image are traversed making a comparison of the gray level (scale that goes from 0 to 255 denoting the light intensity of an image, with 0 representing the completely black color and 255 the white color, with intermediate values representing different levels of gray) of the corresponding pixels in the image to be processed, and the reference [29], [30]. If the corresponding pixels of the processed and reference images are considered similar, that is, they present differences in the gray scale values within a pre-determined range (in the present processing, the pixels that have a difference in their level of gray of up to 25), the pixel is understood as the “background” of the image (that is, a region where there are no microbubbles) and in the processed image this pixel is defined as white (value equal to 255). However, if the corresponding pixels are considered different (gray level difference greater than 25), the pixel is understood to be part of a droplet, and then in the processed image the corresponding pixel is defined as black (value equal to 0). Equation 1 shows the applied logic:

$$f(x) = \begin{cases} 255 & (\text{Original} - \text{Reference}) < 25 \\ 0 & (\text{Original} - \text{Reference}) \geq 25 \end{cases} \quad (\text{Equation 1})$$

Figure 3 presents an example of the original image (a) together with the image obtained after applying the described technique (b). This initial processing provides an image in which the background is white and the droplets are black (binary image, only with values 255 or 0). However, until this stage, normally only the droplet contour regions were identified, leaving a small region in the center still identified as background. In this step, all regions that are surrounded by black (regions that are theoretically in the middle of the interfaces found in a droplet, and therefore are also part of the droplet) they are also filled with black. This procedure is performed using region filling using the “in-fill” function, a function of the MATLAB® image processing library, which uses an algorithm based on morphological reconstruction [30]. With this, an image is obtained in which the droplets are all represented in black and the background of the image all in white. In Figure 3 (c), the image processed in the previous step can be seen, together with the image after applying the “infill” function [31]. In the next step, each of the black regions in the image is identified separately (with values 0), which represent each of the droplets. The feature extraction step, involving the calculation of the area, in pixels, of each of these regions, is performed with the aid of the “regionprops” function in MATLAB®. The different regions considered as individual droplets are shown in Figure 3 (d), with each droplet represented by a different color. Each droplet identified has its diameter in pixels (DP) determined, based on the area in pixels (AP) it occupies (Equation 2).

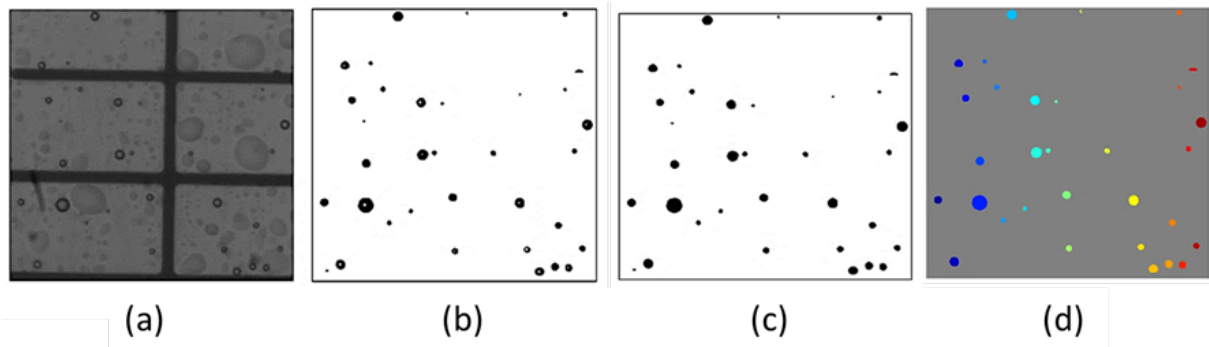


**Figure 3:** (a) Original image; (b) Image obtained after applying the segmentation technique used; (c) Image obtained after the application of the “infill” function and (d) Different regions of different colours are considered individual droplets. Source: Own authorship.

$$D_p = \sqrt{4A_p/\pi} \tag{Equation 2}$$

Areas considered to be very small are disregarded as they represent possible noise from image processing. An example with images before and after eliminating possible noise is shown in Figure 4.

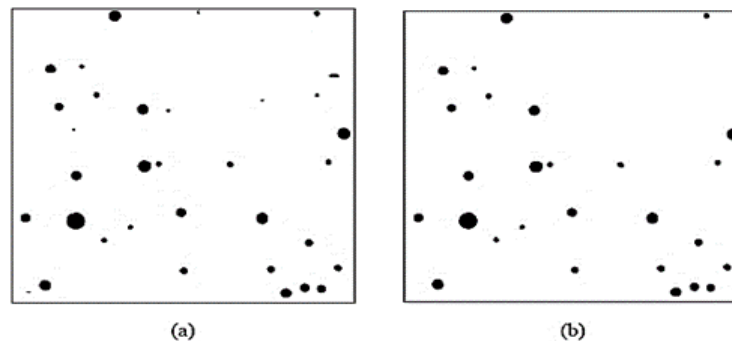


**Figure 4:** (a) Image before eliminating possible noise (b) Image after eliminating possible noise. Source: Own authorship.

The diameters found so far are still in pixels as a unit, so it becomes necessary to convert them to a unit of suitable length for analysis (micrometres, for example). This is done through a reference measurement of the image

using the Stage Micrometer. A real length taken as standard in the image is then measured in pixels, which allows the transformation to be made for all calculated diameters [31]. At this point in the processing, all droplet diameters identified in the image are distributed. What is done next is to create histograms (with the “hist” function) to represent the distribution of the diameters found in the image in the desired way, as shown in Figure 5. The process is then repeated for all images, creating a histogram of diameters for each image. Finally, an additional histogram is created considering now all the droplets found in all the images.

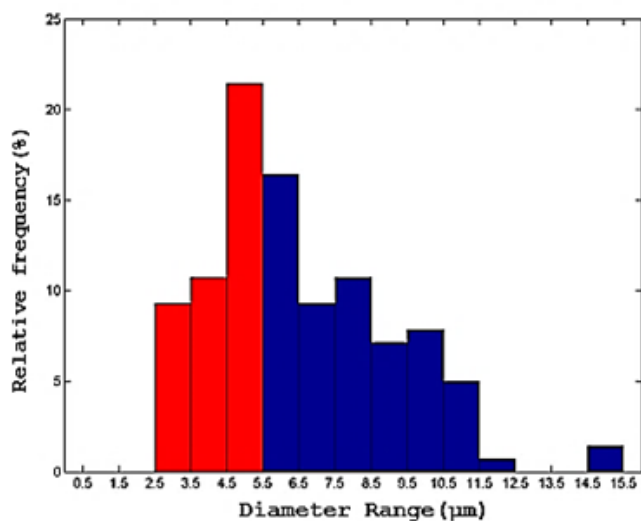


**Figure 5:** Histogram representing the relative frequency as a function of the droplet diameter range. Source: Own authorship.

### 2.3. PHYSICOCHEMICAL AND PHARMACOLOGICAL PROPERTIES OF DRUGS

Physicochemical properties of drugs currently used to treat SARS-CoV-2 signs and symptoms, such as water solubility, acid dissociation constant (pKa), oil/water partition coefficient, molecular mass, granulometry, surface contact area, among others, were compiled into databases PubChem [32] and Drug Bank [33]. Data on physical and chemical constants and data on pharmacokinetics and pharmacodynamics were extracted. In addition, the Brazilian Pharmacopoeia [34] and Brazilian laws were consulted which provide for in vitro performance tests and tests to prove therapeutic equivalence for oral inhaled drugs and nasal sprays and aerosols [35], [36].

## 3. RESULTS AND DISCUSSIONS

The three nebulizers surveyed use the value of the Average Aerodynamic Mass Diameter (MMAD) present in the manuals as a standard for characterizing the droplets. This variable represents the average value of the aerodynamic size of the droplets generated by each of the researched nebulizers, since it takes into account the size of the mass diameter of each drop.

In the development of this work, Median Aerodynamic Diameter Count (CMAD) was used to characterize the size of the aerodynamic dispersion droplets produced by the nebulizers studied here. This parameter represents the median of the droplets, i.e., it characterizes the amount of 50% of the droplets that are above the average and the 50% of the droplets that are below the average. For each of the surveyed nebulizers, a statistical analysis was made of the number of droplets generated as a function of the diameter, and a characteristic histogram related to the droplet diameter was elaborated, emphasizing the range between 1.0 to 5.0 µm which corresponds to the ideal range. Table 1 presents the information about the diameter of the droplets conveyed in the factory manuals, percentage of the droplets located in the ideal range, and characteristic average diameter of the droplets in suspension for each nebulizer (sample) using the parameter (CMAD) using the technique DLI.

**Table 1:** Information on the diameter of the droplets provided by the manuals accompanying the equipment; Percentage of droplets in the ideal range; Characteristic average diameter of the droplets in suspension for each nebulizer (sample) using the parameter (CMAD) using the DLI technique. Source: Own authorship.

Nebulizer	Instruction manual ( $\mu\text{m}$ )	Percentage of particles in the ideal range (%)	CMAD parameter using the DLI technique ( $\mu\text{m}$ )
A	4.0	43.95	5.5
B	<5.0	34.48	5.9
C	0.5-10	58.46	4.5

It can be seen in Table 1 that the information conveyed in the manufacturer’s manuals of the researched nebulizers, brings only the values of the MMAD parameter as a reference, without any information on the methodology used in the determination of that value. In contrast, the table shows the droplet categorization by diameter ranges using the CMAD parameter showing quantitatively the population of droplets located in the ideal range 1.0 to 5.0  $\mu\text{m}$ .

### 3.1. HISTOGRAMS OF NEBULIZERS

Figures 6 to 8 show the histograms of the distribution of the droplets produced by nebulizers A, B and C, from the recording of images captured in the nebulization process in 2.0 s. In each of the histograms, the corresponding range of breathable particles (green bands) is emphasized, that is, droplets with diameters between 1.0 to 5.0  $\mu\text{m}$ .

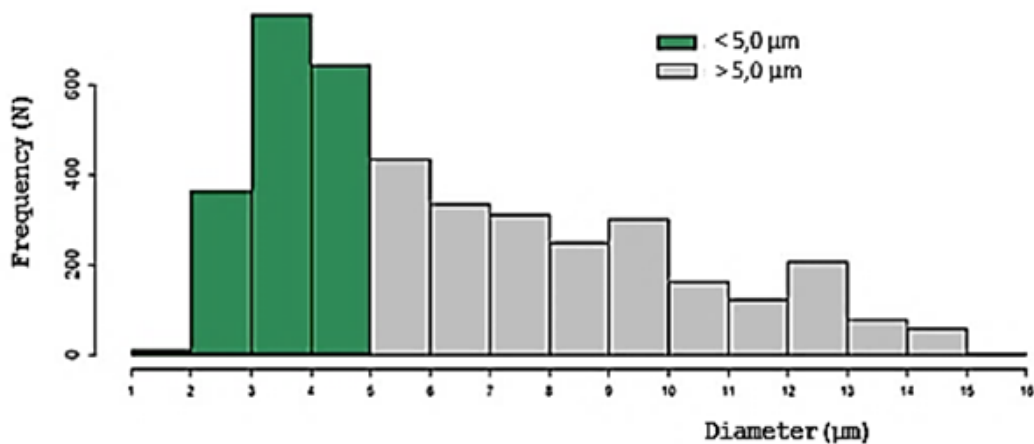


**Figure 6:** Histogram expressing a range of breathable particles from nebulizer A.

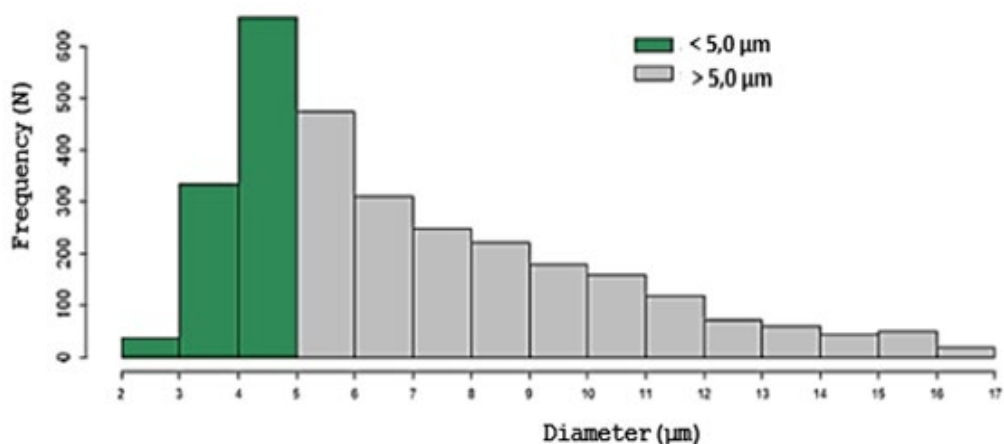


**Figure 7:** Histogram expressing a range of breathable particles from nebulizer B.

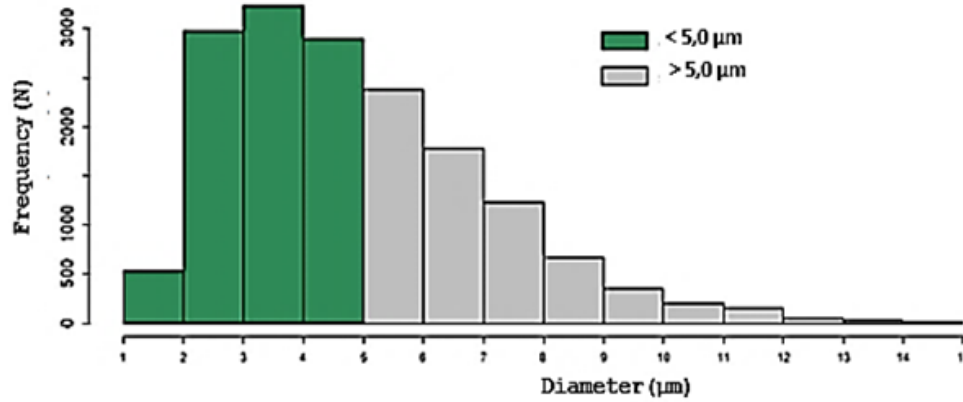


**Figure 8:** Histogram expressing a range of breathable particles from nebulizer C.

Analysing the histograms, it is possible to perceive the polydisperse character of the droplets generated by the nebulizers taken as a sample, and that each equipment has its own characteristic of droplet production in the ideal range (1.0 to 5.0 µm). This represents an important indication for the choice of equipment, since as it has already been treated it is in this range of diameters that a better response to treatment occurs due to a greater effective absorption of the drug by the pulmonary alveoli. The analysis of pure and simple histograms can represent an initial way of characterizing nebulizers based on the ability of each one to deliver droplets in the ideal range.

### 3.2. FREQUENCY DISTRIBUTIONS OF THE DIAMETER OF THE DROPS GENERATED BY THE NEBULIZERS

The histogram with the frequency densities is useful in cases where you want to visualize the fit of the distribution density curves. Each frequency density value (on the vertical axis) is equal to the absolute frequency of the values in the corresponding class (on the horizontal axis), divided by the length of this class. Normal Distribution is widely used in numerous applications with experiments and physical phenomena having symmetry properties around the mean. Although its theoretical model allows positive and negative values of the diameter of droplets, this distribution can be used in practice because low values of standard deviation result in almost zero probabilities of obtaining negative values. The Log Normal, Gamma and Normal Inverse distributions only allow positive values, so there is an interest in using these distributions in experiments that result in only positive values (such as droplet diameters). Another parameter is the Akaike Information Criterion (AIC) criterion of goodness of fit of a set of values to a specific probability distribution: the lower the value of AIC, the better the fit of the model. This criterion verifies the goodness of the adjustment taking into account the number of parameters in the model.

Figures 9 to 11 show the histograms with the frequency densities, associated with the frequency distribution curves: Normal, Log-Normal, Gamma and Inverse Normal for each of the researched nebulizers. These data are of great importance for the characterization of the behaviour of each nebulizer, in addition to the calculation of the important AIC parameter that quantitatively characterizes the correlation between the data.

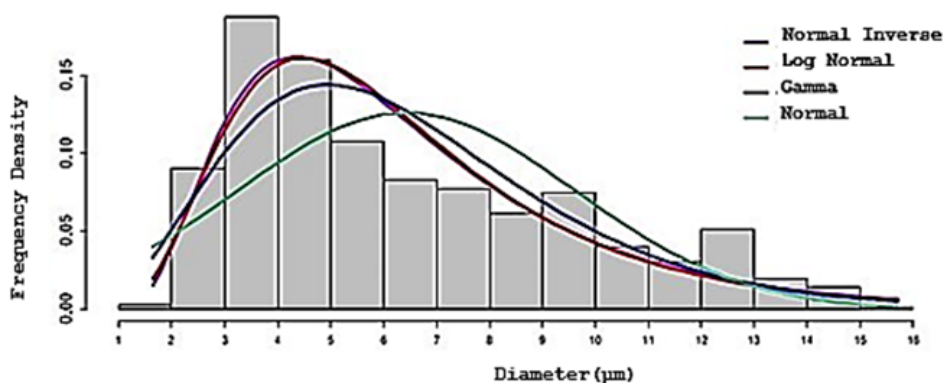


**Figure 9:** Histogram with the density curves adjusted for nebulizer A.



Analysing the graph represented by Figure 9, it can be concluded that the predominance of frequency density in the region between 2.0 and 5.0  $\mu\text{m}$ , is relevant for nebulizer A. In this range there is a large delivery of breathable droplets i.e., (1.0 to 5.0  $\mu\text{m}$ ). It turns out that the Inverse Normal density and Log Normal density curves are almost identical they better capture the modal class of the microbubble diameters (from 3 to 4  $\mu\text{m}$ ).

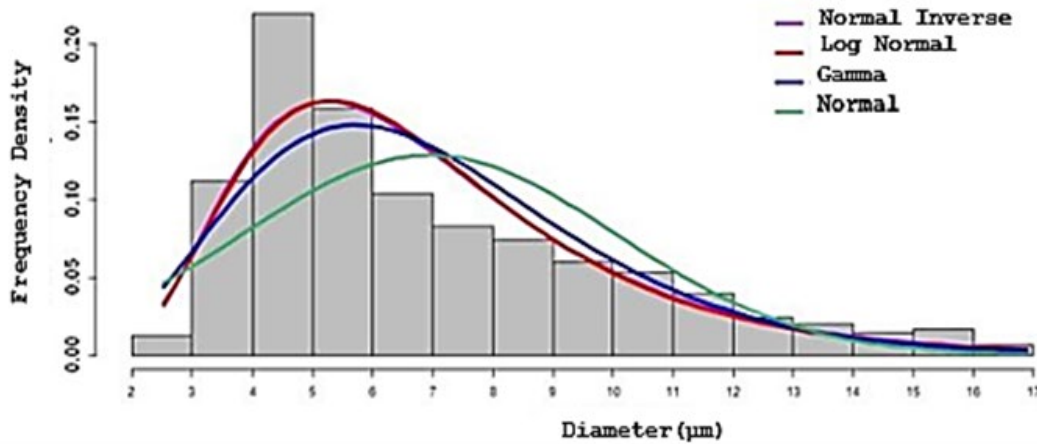


**Figure 10:** Histogram with the density curves adjusted for nebulizer B.

Analysing the graph represented by Figure 10, it is observed that there is a greater concentration of the frequency density distribution in the region between 3.0 and 9.0  $\mu\text{m}$ , with a peak between 4.0 to 5.0  $\mu\text{m}$  for the nebulizer B. It is verified that the Inverse Normal and Log Normal density curves are almost identical, they better capture the modal class of the micro-bubble diameters from 4.0 to 5.0  $\mu\text{m}$ . The graph represented by Figure 45 shows the behaviour of the F nebulizer according to the tested distributions.

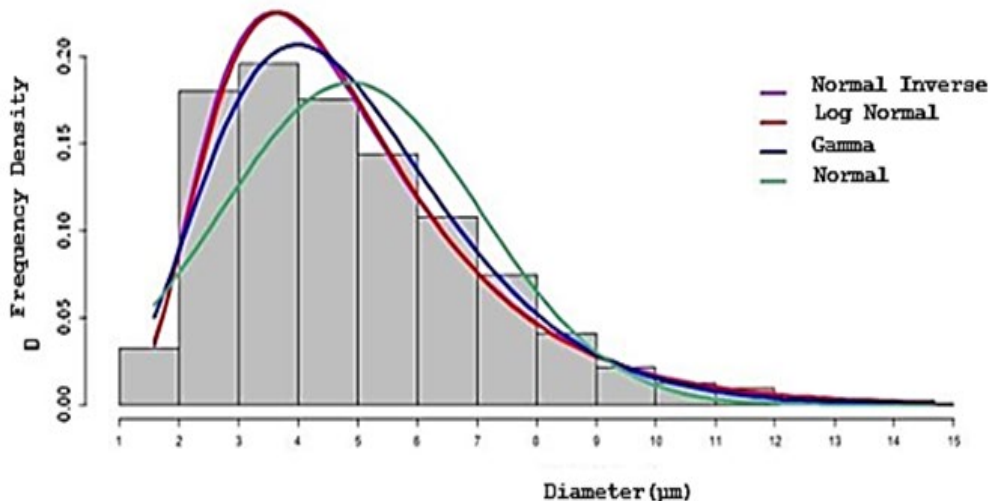


**Figure 11:** Histogram with the density curves adjusted for nebulizer C.

Analysing the graph represented by Figure 11, a peak between 3.0 and 4.0  $\mu\text{m}$  is observed for the F nebulizer. It can be seen that the Inverse Normal and Log Normal density curves are almost identical - they better capture the class modal of the microbubble diameters (from 3.0 to 4.0  $\mu\text{m}$ ), in addition to adjusting better to values close to 1.0  $\mu\text{m}$  (to the left of the graph). From the aspects presented of the adjusted distributions, in above figures, we can verify a summary of the statistical parameters for each nebulizer studied. This analysis shows a predominance of the Log Normal distribution, according to the literature on the distribution that best fits the micro droplet size data. Table 2 shows the Mean, Median, Standard Deviation, and Adjusted Distribution of the data.

**Table 2:** Descriptive statistics with adjusted distributions and Akaike criteria (AIC), in addition to the values relative to Mean, Median, and Standard Deviation.

Nebulizer	Mean	Median	Standard deviation ( $\sigma$ )	Adjusted Distribution
A	6.43	5.51	3.17	Log Normal
B	6.94	5.95	3.09	Log Normal
C	4.88	4.51	2.15	Log Normal

### 3.3. THE DIRECT LAMINAR INCIDENCE (DLI) TECHNIQUE IN THE CHARACTERIZATION OF AERO DISPERSED DROPS

Microscopy is considered an absolute method of analysing particle size, since it is the method in which individual particles are observed and measured [19]. The other analysis techniques such as Laser diffraction (LD), Cascade Impactor (CI), and Phase Doppler Anemometry (PDA) as previously described are calibrated using optical microscopes and high intensity lasers, which characterize indirect measurements [26]. This finding suggests that optical microscopy is more suitable when working with dispersed aero particles with diameters between 0.8 to 150.0  $\mu\text{m}$  depending on the wavelength of the light source, although a practical lower limit of 3.0  $\mu\text{m}$  it is frequently cited [19].

Thus, digital processing of aerosol microscopy images produced by nebulizers can provide reliable results. Based on this information, the microscopic measurement technique was applied as a direct form of measurement associated with image processing, which translates to the DLI technique. Analysing the experimental results, it was found that:

- The histograms presented together with the third column of Table 1, show that each nebulizer has a different behaviour in relation to the delivery of droplets in the ideal region, besides presenting different values of the parameter CMAD. This may be associated with the equipment design or technical anomalies liable to be circumvented by the manufacturers.
- The DLI technique represents a viable alternative for the characterization of aero dispersed droplets, since its operation does not require sophisticated and expensive equipment, which makes it quite competitive in relation to other measurement techniques.
- The difference in behaviour of each nebulizer in delivering droplets in the ideal range, signals that the choice of a certain equipment may present an advantage over the other with regard to the therapeutic response of the treatment, since this response depends on the proportion of droplets in the breathable range, i.e., between 1.0 to 5.0  $\mu\text{m}$  (where the greatest pulmonary deposition).
- The frequency density distribution of the droplet diameter associated with each of their searched nebulizers, shows the high degree of dispersion of the aerodynamic droplet population. This fact is confirmed by the high values of the standard deviations ( $\sigma$ ) associated with each distribution. The proposed methodology with the characterization of the droplets generated by size ranges, introduces a way to evaluate the behaviour of the nebulizers with reference to the ideal region, i.e., 1.0 to 5.0  $\mu\text{m}$ .
- Table 2 shows the behaviour of nebulizers in relation to the statistical data Average, Median, Mode, Standard Deviation, and Adjusted Distribution. It can be seen that there is a predominance of the Log Normal distribution as described in the literature that involves the study of dispersed aero droplets.

### 3.4. PHYSICOCHEMICAL AND PHARMACOLOGICAL PROPERTIES OF DRUGS, WITH POTENTIALS USE BY NEBULIZATION, TO TREAT SARS-CoV-2 SIGNS AND SYMPTOMS

Inhaled drug administration requires attention on application as well as on administration. The physicochemical properties of the formulation and the interactions with the nebulizer were relevant factors, as they can directly affect the properties of the aerosol and, consequently, the bioavailability of the drug and the effectiveness after nebulization [37]. The administration of drug for inhalation is typically associated with high pulmonary efficacy and minimal systemic side effects and, pharmacokinetic processes, such as, drug particle/droplet deposition; pulmonary drug dissolution; absorption to lung tissue; pulmonary tissue retention and tissue metabolism; and, absorptive drug clearance to the systemic perfusion are clinically relevant [38].

One of the proposals of this article is to analysis of the potential of drugs, based on physical-chemical and pharmacological properties, for inhaled administration, as an aid to the multidisciplinary health team, in the treatment of respiratory tract diseases. Tables 3 and 4 show, respectively, the main physical-chemical and pharmacological properties of drugs used in the treatment of respiratory tract diseases, which are currently being investigated to treat SARS-CoV-2 signs and symptoms, worldwide.

So far, there are no vaccines and drugs for the treatment of Coronavirus, however, several countries have been making efforts to create clinical protocols that minimize the damage caused in physiological systems, in human organisms, especially cardiovascular and respiratory damage [39]. Various therapeutic alternatives have been used to treat SARS-CoV-2, among which antimicrobials (Azithromycin and Ciprofloxacin), antimalarials (Chloroquine and Hydroxychloroquine), Antiparasitic (Ivermectin and Nitazoxanide), antirheumatics (Hydroxychloroquine and Tocilizumab), anticoagulants (Enoxaparin and unfractionated Heparin), Non-steroidal anti-inflammatory - NSAID (ibuprofen), Steroidal anti-inflammatory (Prednisolone and Methylprednisolone), antiretrovirals (Lopinavir and Ritonavir), antivirals (Nitazoxanide, Oseltamivir, Remdesivir and Ribavirin). However, often, such drugs are only available in solid (powder, tablet and capsule), semi-solid (suspension) and, some of them, liquid (injectable and ophthalmic) solutions. In the current scenario of the pandemic caused by the Coronavirus, the off-label use of these drugs can be a viable alternative for administration and therapeutic success [40], [41]. In addition, the pharmacotechnical development of new pharmaceutical formulations is a relevant tool, as it encompasses the study of aspects related to chemical substance (drug), pharmaceutical form and industrial technology [42].

The main properties and parameters for pharmaceutical formulations useful for administration via nebulization to be considered when designing an effective inhaler are: aerosol properties (mass median aerodynamic diameter; geometric standard deviation; fine particle fraction and, air/particle velocity); particle properties (volume diameter; bulk density; tap density; shape and, charge); physicochemical properties (solubility and hygroscopicity); and, lung properties (geometry of respiratory tree - airway structure and diameter of airways; influence of disease state on airway structure; breathing pattern - mouth or nasal breathing) [8]. The data obtained showing that the drugs enoxaparin, oseltamivir, ribavirin is the most easily soluble in water. Azithromycin, ibuprofen, prednisolone and methylprednisolone, also show partial solubility in water. Such information about solubility can facilitate its use by inhalation. However, studies of technological and biopharmaceutical feasibility are necessary to obtain stable and effective formulations.

Regarding the molecular mass (MM), a range of 307.28 to 748.98 g/mol (Daltons) is observed for the evaluated drugs. Enoxaparin has a molecular mass between 3,800 to 5,000 Daltons. In this context, the lower the molecular mass, the transport of the molecule through the respiratory tract can be accelerated, reaching the bronchial tree with greater speed and, therefore, being more available for absorption. Ibuprofen, ribavirin and nitoxamide have MM lower than 300 g/mol, which strengthen the possibility of using this route. However, several other physicochemical parameters must be analysed for potential pharmaceutical formulations, suitable for this purpose.

Oil/water partition coefficient (OAPC) is used in drug design as a measure of a solute's hydrophobicity and a proxy for its membrane permeability [43]. In pharmaceutical industry, to estimate how a drug may transfer between different biological environments and are regularly used to predict a molecule's hydrophobicity [44]. Lower OAPC, less the solubility, in fats, of chemical substances. Drugs such as ciprofloxacin, enoxaparin, prednisolone, methylprednisolone, nitazoxamide, oseltamivir, remdesevir and ribavirin have a partition strength of less than 3 and, this can strengthen its use by inhalation, carried in 0.9% saline solution. A pharmacotechnical alternative for the formulation of drugs for use by inhalation would be the incorporation into liposomes. However, some drugs, when diluted in a larger volume, either in a nebulization chamber or even in the lung, such as corticosteroids in liposomes, tend to lose their content in a biphasic pattern determined by their partition coefficient [45].

All the drugs studied had a surface area of less than 250 angstrom, that is, between 0.003 and 0.02  $\mu$ . In this way, drugs used worldwide to treat SARS-CoV-2 signs and symptoms could be transported by nebulization. In this study, DLI technique represents a viable alternative for the characterization of aero dispersed droplets, for administration of these drugs. However, according to data in table 4, some drugs have bioavailability below 40%, with lopinavir (25%) and azithromycin (37%) standing out. In addition, aspects of safety in the use of drugs should be evaluated. Among the main adverse effects are Cardiotoxicity (azithromycin, ciprofloxacin, chloroquine and hydroxychloroquine) and toxic to the respiratory tract (ibuprofen, lopinavir, remdesevir, ritonavir and tocilizumab).

The drugs nitazoxamide and oseltamivir are the least toxic and, therefore, may be potential drugs to be administered by nebulization. In the literature, some studies indicate the inhaled use of Azithromycin [7],

Ciprofloxacin in the treatment of non-cystic fibrosis bronchiectasis [46], Enoxaparin [47], Prednisolone [48], Ribavirin in Chronic Obstructive Pulmonary Disease [49] and Oseltamivir as influenza prophylaxis [50], [51]. Nitazoxanide is related, in literature, as a new drug candidate for the treatment of Middle East respiratory syndrome coronavirus [52]. For treatment of SARS-CoV-2 signs and symptoms, the literature indicated the Hydroxychloroquine as an aerosol might markedly reduce and even prevent severe clinical symptoms infection [53]. In addition, benefit of the Remdesivir for treatment of Coronavirus symptoms, by combination of pulmonary and intravenous administration were studied [54].

In this context, the possibility of innovative treatments for SARS-CoV-2 signs and symptoms is a real necessity and the inhalation route is a potential alternative. Therefore, it is relevant to know the physicochemical properties of drugs already used in clinical practice, which may have the possibility of administration by nebulization.

**Table 3:** Physic-chemical properties of drugs used in diseases of the respiratory tract and, currently being investigated to treat SARS-CoV-2 signs and symptoms [32], [33], [34].

Drug	Pharmaceutical forms available in Brazil	Solubility	Water Solubility (mg/L, at 25 °C)	Molecular mass (Daltons)	Oil / water partition coefficient	Area superficial (Å)	pKa
Azithromycin	tablets, oral suspension and solution for injection	soluble in ethanol and Dimethyl sulfoxide (DSMO)/minimally soluble in water	2.37	748.98	3.03	180.08	8.5
Ciprofloxacin	tablets, solution for injection and ophthalmic solution	Practically insoluble in water. Soluble in dilute acetic acid, very poorly soluble in ethyl alcohol.	$< 1 \times 10^{-3}$	331.34	0.28	72.88	6.09 (carboxylic acid group); 8.74 (nitrogen, in the piperaziny ring)
Chloroquine	tablets (diphosphate) and solution for injection (hydrochloride)	Very little soluble in water. Soluble in diluted acids.	0.14	319.87	4.63	28.16	10.1
Hydroxychloroquine	tablets	NR	$2.61 \times 10^{-4}$	434.0	3.6	48.4	9.67
Enoxaparin	solution for injection (subcutaneous)	soluble in water, alcohol, ether, acetone, chloroform and benzene. Hygroscopic powder.	$> 0.2$	3800 – 5000	-13.2	NR	NR
Ibuprofen	tablets and oral suspension	Practically insoluble in water, easily soluble in ethyl alcohol and alcohol methyl. Soluble in aqueous solutions of	21	206.29	3.97	37.3	5.3

		alkaline hydroxides.					
Ivermectin	tablets	insoluble in water	insoluble	875.1	4.1	170.06	12.47
Lopinavir	tablets	Practically insoluble in water, soluble in methanol and ethanol; soluble in isopropanol	$7.7 \times 10^{-3}$	628.8	5.94	120	13.39
Prednisolone	solution for injection and oral suspension	Moderately soluble in dioxane, methanol; slightly soluble in methanol, acetone, chloroform	223	360.4	1.6	94.8	NR
Methylprednisolone	solution for injection	Moderately soluble in dioxane, methanol; slightly soluble in acetone, chloroform; very slightly soluble in ether.	120	374.5	1,525	94.83	12.59
Nitazoxanide	tablets and oral suspension	NR	0.000189	307.28	1.63	142	8.3
Oseltamivir	capsules and powder for oral suspension	soluble in water	$6.86 \times 10^{-4}$	312.4	1.1	90.65	7.7
Remdesivir	solution for injection	NR	$3,39 \times 10^{-4}$	602.6	2.2	203.55	10.23
Ritonavir	tablets and oral solution	Freely soluble in methanol and ethanol; soluble in isopropanol.	$1.26 \times 10^{-4}$	720.9	3.9	145.78	13.68
Ribavirin	tablets and suspension for injection (subcutaneous)	soluble in water and slightly soluble in alcohol	$\geq 0.1$	244.2	-1.9	143.72	11.88

**Table 4:** Pharmacological properties of drugs used in diseases of the respiratory tract and, currently being investigated to treat SARS-CoV-2 signs and symptoms [32], [33], [34].

Drug	Therapeutic class	Pharmacokinetic processes				Main adverse effects
		Absorption / Bioavailability	Distribution	Metabolism	Elimination	
Azithromycin	Antibiotic (macrolide)	Not affected by food; OB: 37%	Widely distributed in tissues; VD: 31.1 L/Kg; $T_{1/2}$ : approx. 68 hours; BPP: 7-51 %	Hepatic (CYP 3A4)	Bile (main route) - drug unaltered) / Urine (6%)	Thrombocytopenia, arrhythmias (ventricular tachycardia)
Ciprofloxacin	Antibiotic (fluoroquinolone)	OB: 70-80 %	VD: 2.00-3.04 L/Kg; $T_{1/2}$ : 4 hours; BPP: 20-40%	Hepatic (CYP 1A2)	Urine (45%) and feces (62%)	Tachycardia, dyspnoea, thrombocytopenia

Nebulizers: Aerodynamic Droplet Diameter Characterization and Physicochemical Properties of Drugs to Treat Severe Acute Respiratory Syndrome Corona Virus 2 (Sars-Cov-2)

Chloroquine	Antimalarial	OB: 67-114 %	VD: 200-800 L/Kg; T <sub>1/2</sub> : 20-60 days; BPP: 46-74%	Hepatic (CYP 2C8, CYP 3A4, CYP 3A5, CYP 2D6 and CYP 1A1)	Urine (50% unaltered)	Cardiotoxicity (atrioventricular block, cardiomyopathies)
Hydroxychloroquine	Antimalarial and Antirheumatic	OB: 67-74%	VD: 5,522 L/Kg (blood); 44,257 L/Kg (plasma); T <sub>1/2</sub> : 537 hours (blood); 2,963 hours (plasma); BPP: 50%	Hepatic (CYP 3A4)	Renal (40-50%); urine (16-21%) / skin (5%) and feces (24-25%)	Cardiomyopathy, prolongation of QT interval, emotional lability
Enoxaparin	Anticoagulant	100 %	VD: 4.3 L/Kg; T <sub>1/2</sub> : 4.5 hours; BPP: 80 %	Hepatic (desulfation and polymerization)	Urine (40% of the dose)	Haemorrhages, thrombocytopenia, haematuria
Ibuprofen	Non-steroidal anti-inflammatory	OB: 80-90 %	VD: 0.1 L/Kg; T <sub>1/2</sub> : 1.2 - 2 hours; BPP: 99 %	Hepatic (CYP 2C9)	Urine (90%)	Bronchospasm, CHF, gastrointestinal disorders, hypertension, anaphylaxis
Ivermectin	Antiparasitic	absorption moderate, especially with a diet rich in fats	VD: 3.5 L/Kg; T <sub>1/2</sub> : 16 hours; BPP: 93 %	Hepatic	Feces	Diarrhea, nausea, urticaria, onchocerciasis, hypotension
Lopinavir	Antiretroviral	OB: 25%	VD: 16.9 L/Kg; T <sub>1/2</sub> : 6.9 ± 2.2 hours; BPP: > 98 %	Hepatic (CYP 3A4)	Feces	SRT infections, diarrhea, anemia, angioedema
Prednisolone	Steroidal anti-inflammatory	70 %	VD: 29.3 L/Kg; T <sub>1/2</sub> : 2.1-3.5 hours; BPP: 70-90 %	Hepatic	Urine (98 %)	CHF, arrhythmias, leukocytosis, cushing's syndrome, hypopituitarism
Methylprednisolone (MP)	Steroidal anti-inflammatory	OB: MP acetate (89.9%) and rectal (14.2%)	VD: 1.38 L / Kg; T <sub>1/2</sub> : 2.3 hours; BPP: 76.8 %	Hepatic	Urine	
Nitazoxanide	Antihelmintic and Antiviral	70 % (suspension)	VD: not found; T <sub>1/2</sub> : 7.3 hours; BPP: > 99)	Hepatic	Urine, bile and feces.	abdominal colic, diarrhea, headache
Oseltamivir	Antiviral	OB: 75 %	VD: 23-26 L/Kg; T <sub>1/2</sub> : 1-3 hours; BPP: 42 %	Hepatic	Renal (90 %).	Nausea, vomiting, headache and body pains

Remdesivir	Antiviral	NR	VD: NR; T <sub>1/2</sub> : 20 hours (metabolite) ; BPP: NR	NR	Urine (74 %) and feces (18 %)	RF, hypotension
Ritonavir	Antiretroviral	NR	VD: 0.41 ± 0.25 L/Kg; T <sub>1/2</sub> : 1-3 hours; BPP: > 98 %	Hepatic (CYP3A4 and CYP2D6)	Feces (86 %).	IRT, cellulite, folliculitis and furunculosis
Ribavirin	Antiviral	OB: 45-64 %	VD: NR; T <sub>1/2</sub> : 120- 170 hours; BPP: NR	Renal	Urine (61 %) and feces (12 %)	Anemia, anorexia, depression
Tocilizumab	Antirheumatic	80-96 %	VD: 6.4 L / Kg; T <sub>1/2</sub> : 11 - 13 days; BPP: NR	Hepatic	Renal (linear deuration)	SRT infections, leukopenia

OB: Oral bioavailability; VD: apparent volume of distribution; BPP: Binding to plasmatic proteins; T<sub>1/2</sub>: Time oh half-life; NR (not reported); CHF: Congestive Heart Failure; Superior Respiratory Tract (SRT); Inferior Respiratory Tract (IRT); MP: Methylprednisolone; RF: Respiratory failure.

## 6. CONCLUSIONS AND RECOMMENDATIONS

The quantification of the diameter of the droplets produced by the nebulizers taken as a sample using DLI technique led to the elaboration of the characteristic histograms of each nebulizer researched, relating the frequency of events as a function of the droplet diameter. In the histograms presented, the ideal range corresponding to the breathable droplets was emphasized, that is, those with diameters between 1.0 to 5.0 µm. Allied to that, graphs of the histograms associated with the Normal, Log distribution curves Normal, Gamma and Inverse Normal to assess the most appropriate type of distribution according to with the database. It was concluded that the distribution that comes closest is Log Normal according to the literature dealing with the topic under study. The polydispersed character of the population of the droplets generated by the nebulizers was also proven, attested by the high Deviation Standard ( $\sigma$ ) of the diameters related to the mean.

The choice of CDMA over MMAD arose from the need to use a parameter alternative to quantify the population of breathable droplets, CDMA made this possible because it works with the representation of the median of the droplets, and not a value absolute mean mass diameter of the droplet population represented by MMAD.

DLI technique proved to be efficient for the characterization of dispersed aero droplets, combining optical procedures aimed at image acquisition, computational processing techniques. In addition, it proved to be operationally viable for its simple and accessible character by using low cost materials and equipment compared to the other techniques already mentioned.

The question raised at the beginning of the work regarding the qualification of efficiency nebulizers to deliver droplets with diameters between 1.0 to 5.0 µm, which corresponds to the range of breathable droplets, was answered according to the results experimental results achieved. This parameter is of fundamental importance, as it provides a differentiation of nebulizers according to their ability to deliver droplets in the range above, which provides a better therapeutic response during inhalation treatment.

In this scenario, there is still much to speculate in the search for an effective, accessible and safe therapeutics for use to treat SARS-CoV-2 signs and symptoms. Knowledge of physicochemical and pharmacological properties is essential for the development of new innovative formulations for administration by inhalation. DLI technique represents a viable alternative for the characterization of aero dispersed droplets, for administration of these drugs.

## SOURCES OF FUNDING

This research received no specific grant from any funding agency in the public, commercial, or not-for-profit sectors.

## CONFLICT OF INTEREST

The author have declared that no competing interests exist.

## ACKNOWLEDGMENT

The authors are grateful for State University of Bahia (UNEB), “Coordenação de Aperfeiçoamento de Pessoal de Nível Superior – Brasil (CAPES)” and Research Group: Biopharmaceutics and Drugs.

## REFERENCES

- [1] Kiselev, D., Matsvay, A., Abramov, I., Dedkov, V., Shipulin, G. and Khafizov, K. Current Trends in Diagnostics of Viral Infections of Unknown Etiology, *Viruses*. **12**, 2020, 211.
- [2] Woolhouse, M., Scott, F., Hudson, Z., Howey, R. and Chase-Topping, M. Human viruses: Discovery and emergence, *Philosophical Transactions of the Royal Society B: Biological Sciences*. **367**, 2012, 2864–2871.
- [3] Hasan, S., Ahmad, S. A., Masood, R. and Saeed, S. Ebola virus: A global public health menace: A narrative review, *Journal of Family Medicine and Primary Care*. **8**, 2019, 2189–2201.
- [4] Kazmi, S. S., Ali, W., Bibi, N. and Nouroz, F. A review on Zika virus outbreak, epidemiology, transmission and infection dynamics, *Journal of Biological Research-Thessaloniki*. **27**, 2020, 5.
- [5] McBride, R. and Fielding, B.C. The Role of Severe Acute Respiratory Syndrome (SARS)-Coronavirus Accessory Proteins in Virus Pathogenesis, *Viruses*. **4**, 2012, 2902–2923.
- [6] Astuti, I. and Ysrafil. Severe Acute Respiratory Syndrome Coronavirus 2 (SARS-CoV-2): An overview of viral structure and host response, *Diabetes & Metabolic Syndrome: Clinical Research & Reviews*. **14**, 2020, 407–412.
- [7] Mangal, S., Nie, H., Xu, R., Guo, R., Cavallaro, A., Zemlyanov, D. and Zhou, Q. Physico-Chemical Properties, Aerosolization and Dissolution of Co-Spray Dried Azithromycin Particles with L-Leucine for Inhalation, *Pharmaceutical Research*. **8**, 2018, 28.
- [8] Ibrahim, M., Verma, R. and Garcia-Contreras, L. Inhalation drug delivery devices: technology update, *Medical devices (Auckland, N.Z.)*. **8**, 2015, 131–139.
- [9] Tsuda, A., Henry, F. S. and Butler, J. P. Particle transport and deposition: basic physics of particle kinetics, *Comprehensive Physiology*. **3**, 2013, 1437–1471.
- [10] Anderson, P. J. History of Aerosol Therapy: Liquid Nebulization to MDIs to DPIs, *Respiratory Care*. **50**, 2005, 1139–1150.
- [11] Ari, A., Hess, D., Myers, T. R. and Rau, J. L. A guide to aerosol delivery devices for respiratory therapists. 2<sup>nd</sup>. Dallas, Texas: American Association for Respiratory Care, 2009.
- [12] Amirav, I., Balanov, I., Gorenberg, M., Groshar, D. and Luder, A. S. Nebulizer hood compared to mask in wheezy infants: aerosol therapy without tears!, *Archives of Disease in Childhood*. **88**, 2003, 719–723.
- [13] Tena, A. F., Clarà, P. C. Deposition of Inhaled Particles in the Lungs, *Archivos de Bronconeumología*. **48**, 2012, 240–246.
- [14] Carvalho, T. C., Peters, J. I. and Williams 3rd, R. O. Influence of particle size on regional lung deposition – What evidence is there? *International Journal of Pharmaceutics*. **406**, 2011, 1–10.
- [15] Willeke, K. and Baron, P. A. Aerosol Measurement - Principles, Techniques and Applications: An Nostrand Reinhold, New York, 1993.
- [16] Ho, K. K. L., Kellaway, I.W. and Tredree, R. L. Particle size analysis of nebulized aerosols using Fraunhofer laser diffraction and inertial impaction methods, *Journal of Pharmacy and Pharmacology*. **38**, 1986, S26P.



- [17] Patton, J. S. and Byron, P. R. Inhaling medicines: delivering drugs to the body through the lungs, *Nature Reviews Drug Discovery*. **6**, 2007, 67–74.
- [18] Bennet, W. D. Aerosolized drug delivery: fractional deposition of inhaled particles, *Journal of Aerosol Medicine*. **4**, 1991, 223–227.
- [19] Allen T. Powder Sampling and Particle Size Determination, Elsevier Press, Amsterdam, Netherland. 2003.
- [20] Yeo, L. Y., Friend, J. R., McIntosh, M. P., Meeusen, E. N. T. and Morton, D. A. V. Ultrasonic nebulization platforms for pulmonary drug delivery, *Expert Opinion on Drug Delivery*. **7**, 2010, 663–679.
- [21] Dolovich, M. Measurement of particle size characteristics of metered dose inhalers (MDI) aerosols, *Journal of Aerosol Medicine*. **4**, 1991, 251–263.
- [22] Porstendörfe, J., Gebhart, J. and Riöbig, G. Effect of Evaporation on the Size Distribution of Nebulized Aerosols, *Journal of Aerosol Science*. **8**, 1977, 371–380.
- [23] Dolovich, M. B. and Dhand. R. Aerosol drug delivery: developments in device design and clinical use, *Lancet*. **377**, 2011, 1032–1045.
- [24] Kippax, P. Measuring Particle Size Using Modern Laser Diffraction Techniques, *Paint & Coatings Industry Magazine*. **21**, 2005, 42–47.
- [25] Araújo, L. M. P., Abatti, P. J., Araújo Filho, W. D. and Alves, R. F. Performance evaluation of nebulizers based on aerodynamic droplet diameter characterization using the Direct Lamina Incidence (DLI), *Research on Biomedical Engineering*. **33**, 2017, 105–112.
- [26] O’Callaghan, C. and Barry, P. W. The science of nebulised drug delivery, *Thorax*. **52**, 1997, 31–44.
- [27] De Boer, A. H., Gjaltema, D., Hagedoorn, P. and Frijlink, H. W. Characterization of inhalation aerosols: a critical evaluation of cascade impactor analysis and laser diffraction technique, *International Journal of Pharmaceutics*. **249**, 2002, 219–231.
- [28] Durst F., Melling, A. and Whitelaw, J. H. Principles and practice of laser-Doppler anemometry, Academic Press, 1981.
- [29] Zhou, H., Wu, J. and Zhang, J. Digital Image Processing: Part I. Bookboon, 2010.
- [30] Soille, P. Morphological Image Analysis: Principles and Applications, Springer-Verlag, 1999.
- [31] Gonzalez, R. C. and Woods, R. E. Digital Image Processing, Prentice-Hall, Upper Saddle River, NJ, 2002.
- [32] PUBCHEM, United States of America. (2020). Retrieved from: <https://pubchem.ncbi.nlm.nih.gov/compound>.
- [33] DRUG BANK, Canadá. (2020). Retrieved from: <https://www.drugbank.ca/drugs>.
- [34] Brazilian Pharmacopeia, 6th ed.; Brasília: Brazilian Health Surveillance Agency; 2019.
- [35] Ministry of Health, Brazilian Health Surveillance Agency (ANVISA). Normative Instruction No. 33. Brasília. (2019). Retrieved from: [http://portal.anvisa.gov.br/documents/10181/3178137/IN\\_33\\_2019\\_pdf/bf52c1a2-aa89-4b94-9001-98c457777e93](http://portal.anvisa.gov.br/documents/10181/3178137/IN_33_2019_pdf/bf52c1a2-aa89-4b94-9001-98c457777e93).
- [36] Ministry of Health, Brazilian Health Surveillance Agency (ANVISA). Resolution of the Board of Directors – RDC No. 278. Brasília. (2019). Retrieved from: [http://portal.anvisa.gov.br/documents/10181/3178137/RDC\\_278\\_2019\\_pdf/69422274-3489-44b9-83d8-88b2044cc147](http://portal.anvisa.gov.br/documents/10181/3178137/RDC_278_2019_pdf/69422274-3489-44b9-83d8-88b2044cc147).
- [37] Mansour, H. M. Inhaled medical aerosols by nebulizer delivery in pulmonary hypertension, *Pulmonary Circulation*. **8**, 2018, 2045894018809084.
- [38] Borghardt, J. M., Kloft, C. and Sharma, A. Inhaled Therapy in Respiratory Disease: The Complex Interplay of Pulmonary Kinetic Processes, *Canadian Respiratory Journal*. **2018**, 2018, 2732017.
- [39] Zhang, Y., Geng, X., Tan, Y., Li, Q., Xu, C., Xu, J., Hao, L., Zeng, Z., Luo, X., Liu, F. and Wang, H. New understanding of the damage of SARS-CoV-2 infection outside the respiratory system, *Biomedicine & Pharmacotherapy*. **127**, 2020, 110195.
- [40] Alper, J. D. and Gertner, E. Off-Label Therapies for COVID-19—Are We All In This Together?, *Clinical Pharmacology & Therapeutics*. 2020, 10.1002/cpt.1862. “in press.”
- [41] Romani, L., Tomino, C., Puccetti, P. and Garaci, E. Off-label therapy targeting pathogenic inflammation in COVID-19, *Cell Death Discovery*. **6**, 2020, 49.
- [42] Pramod, K., Tahir, M. A., Charoo, N. A., Ansari, S. H. and Ali, J. Pharmaceutical product development: A quality by design approach. *International Journal of Pharmaceutical Investigation*. **6**, 2016, 129–138.

- [43] Bannan, C. C., Calabró, G., Kyu, D. Y. and Mobley, D. L. Calculating partition coefficients of small molecules in octanol/water and cyclohexane/water, *Journal of Chemical Theory and Computation*. **12**, 2016, 4015–4024.
- [44] Sangster, J. J. Octanol-Water Partition Coefficients of Simple Organic Compounds, *Journal of Physical and Chemical Reference Data*. **18**, 1989, 1111–1227.
- [45] Labiris, N. R. and Dolovich, M. B. Pulmonary drug delivery. Part II: The role of inhalant delivery devices and drug formulations in therapeutic effectiveness of aerosolized medications, *British Journal of Clinical Pharmacology*. **56**, 2003, 600–612.
- [46] Chorepsima, S., Kechagias, K. S., Kalimeris, G., Triarides, N. A. and Falagas, M. E. Spotlight on inhaled ciprofloxacin and its potential in the treatment of non-cystic fibrosis bronchiectasis, *Drug Design, Development and Therapy*. **12**, 2018, 4059–4066.
- [47] Bai, S.; Thomas, C.; Ahsan, F. Dendrimers as a carrier for pulmonary delivery of enoxaparin, a low-molecular weight heparin. *Journal of Pharmaceutical Sciences*. **96**, 2007, 2090–2106.
- [48] Daley-Yates, P. T. Inhaled corticosteroids: potency, dose equivalence and therapeutic index, *British Journal of Clinical Pharmacology*. **80**, 2015, 372–380.
- [49] Dumont, E. F., Oliver, A. J., Ioannou, C., Billiard, J., Dennison, J., Van den Berg, F., Yang, S., Chandrasekaran, V., Young, G. C., Lahiry, A., Starbuck, D. C., Harrell, A. W., Georgiou, A., Hopchet, N., Gillies, A. and Baker, S. J. A Novel Inhaled Dry-Powder Formulation of Ribavirin Allows for Efficient Lung Delivery in Healthy Participants and Those with Chronic Obstructive Pulmonary Disease in a Phase 1 Study. *Antimicrobial Agents and Chemotherapy*. **64**, 2020, e02267-19.
- [50] Aekthananon, T., Pukritayakamee, S., Ratanasuwan, W., Jittamala, P., Werarak, P., Charunwatthana, P., Suwanagool, S., Lawpoolsri, S., Stepniewska, K., Sapchookul, P., Puthavathana, P., Fukuda, C., Lindegardh, N., Tarning, J., White, N. J., Day, N. and Taylor, W. R. J. Oseltamivir and inhaled zanamivir as influenza prophylaxis in Thai health workers: a randomized, double-blind, placebo-controlled safety trial over 16 weeks, *Journal of Antimicrobial Chemotherapy*. **68**, 2013, 697–707.
- [51] Leyva-Gradoa, V. H. Palese, P. Aerosol administration increases the efficacy of oseltamivir for the treatment of mice infected with influenza viruses, *Antiviral Research*. **142**, 2017, 12–15.
- [52] Rossignol, J. F. Nitazoxanide, a new drug candidate for the treatment of Middle East respiratory syndrome coronavirus, *Journal of Infection and Public Health*. **9**, 2016, 227–230.
- [53] Klimke, A., Hefner, G., Will, B. and Vossa, U. Hydroxychloroquine as an aerosol might markedly reduce and even prevent severe clinical symptoms after SARS-CoV-2 infection, *Medical Hypotheses*. **142**, 2020, 109783.
- [54] Sun, D. Remdesivir for Treatment of COVID-19: Combination of Pulmonary and IV Administration May Offer Additional Benefit, *The AAPS Journal*. **22**, 2020, 77.